



Design of cold-formed steel built-up nested columns subject to flexural buckling

Akshay Mangal Mahar¹, S. Arul Jayachandran², Mahen Mahendran³

Abstract

Cold-formed steel (CFS) built-up columns are widely used nowadays. The North American design standard (NAS 2016) suggests using a modified slenderness ratio (MSR) for CFS built-up columns undergoing elastic flexural buckling. The existing MSR applies to sections in which the screw fasteners experience shear, and hence this recommendation excludes the use of nested built-up columns. An improved slenderness ratio (ISR) is proposed in this study for the nested built-up columns made of two channels. For this, the exact buckling stress results of a compound spline finite strip method (CoSFSM) based computational tool has been used as the basis. The CoSFSM tool was developed to account for the effect of screw fasteners on the buckling behaviour of built-up section columns. The proposed ISR equation is developed by generating a suitable curve-fitting equation based on a numerical study. For this purpose, a finite element model is developed and validated using the test results available in the literature on long CFS built-up nested channel columns. The obtained ultimate strength results are used to investigate the NAS (2016) based design predictions with the buckling stress results of CoSFSM, and the existing MSR suggested in NAS (2016). This is the first time the exact buckling stress solutions are used to evaluate the NAS (2016) recommendation for the nested built-up columns subject to flexural buckling. The proposed ISR will help the design engineers obtain accurate flexural buckling strengths of CFS built-up nested columns.

1. Introduction

Cold-formed steel (CFS) built-up section columns are used extensively for relatively large spans and high loads. Compared to single open CFS sections, face-to-face connected built-up nested sections show high torsional and flexural rigidity. For the design of built-up section columns, the North American Standard (NAS 2016) suggests using a modified slenderness ratio (MSR) (Eq. 1). But the MSR is limited to sections where the connecting screw fasteners experience shear during flexural deformation. For built-up nested sections, the connecting screws will be on the plane of the neutral axis; thus, these sections do not qualify the criteria of using the MSR of NAS (2016). In this study, the applicability of MSR for the elastic flexural buckling stress ($f_{cr,g}$) prediction and its impact on the ultimate load prediction of built-up nested section column is explored.

¹ Joint PhD Research Scholar, IIT Madras and QUT, Australia, <akshaymangal.mahar@hdr.qut.edu.au>

² Professor, Indian Institute of Technology Madras, India, <aruls@civil.iitm.ac.in>

³ Professor, Queensland University of Technology, Australia, <m.mahendran@qut.edu.au>

The modified slenderness ratio (MSR) is given as,

$$\left(\frac{KL}{r}\right)_{MSR} = \sqrt{\left(\frac{KL}{r}\right)_o^2 + \left(\frac{s}{r_i}\right)^2} \quad (1)$$

where $(KL/r)_o$ is the slenderness ratio of the fully-composite section; s is the fastener spacing; and r_i is the radius of gyration of the single section.

2. Literature Review

Whittle and Ramseyer (2009) and Reyes and Guzman (2011) conducted compression tests on built-up face-to-face sections connected by seam welds. They concluded that the design strength equations of AISI-S100 (2007), when used with the modified slenderness ratio (MSR), would lead to conservative strength predictions. Young and Chen (2008) performed tests on the built-up box section connected using screw fasteners, and DSM based modified design procedures for the strength prediction of built-up box sections was proposed. Li et al. (2014) suggested that torsional or flexural-torsional failure mode shall be neglected if the built-up nested section fails about its symmetry axis, based on their experimental and numerical studies. Roy et al. (2019) suggested that the NAS (2016) design guidelines over-predict the strength by 17% for built-up nested section columns. Vy and Mahendran (2021) recently performed experimental and numerical studies on the built-up nested section columns. They concluded that the fastener spacing did not significantly affect the ultimate capacity and proposed a DSM-based design procedure.

In the above studies, the elastic flexural buckling stress (f_{crg}) of built-up nested section columns was calculated using approximate methods; thus, discrepancies were reported while comparing with the test results. Hence, there is a need to validate the design strength equation of NAS (2016) based on the actual elastic flexural buckling stress solutions.

3. Details of Finite Element Modelling

The finite element software ABAQUS (2021) was used in this study to develop the finite element models of built-up nested sections made of two lipped channels. The four-node shell element with reduced integration (S4R) was selected in the FE model to create the mid-plane geometry. The S4R elements are used in the literature to analyze CFS built-up members (Zhang and Young 2018, Mahar et al. 2021, and Vy and Mahendran 2021). The mesh size of 5 mm × 5 mm was selected based on the studies of Zhang and Young (2018) and Vy and Mahendran (2021) on the built-up nested section columns.

The load and boundary conditions were applied through a reference point formed at the section's centroid. Multi-point connector (MPC) beam elements were used to connect the reference points with the member ends to apply uniform stress and warping constraints, as shown in Fig. 1. These reference points will behave as the control points for the simulation of different boundary conditions, i.e., pin-ends or fixed-ends.

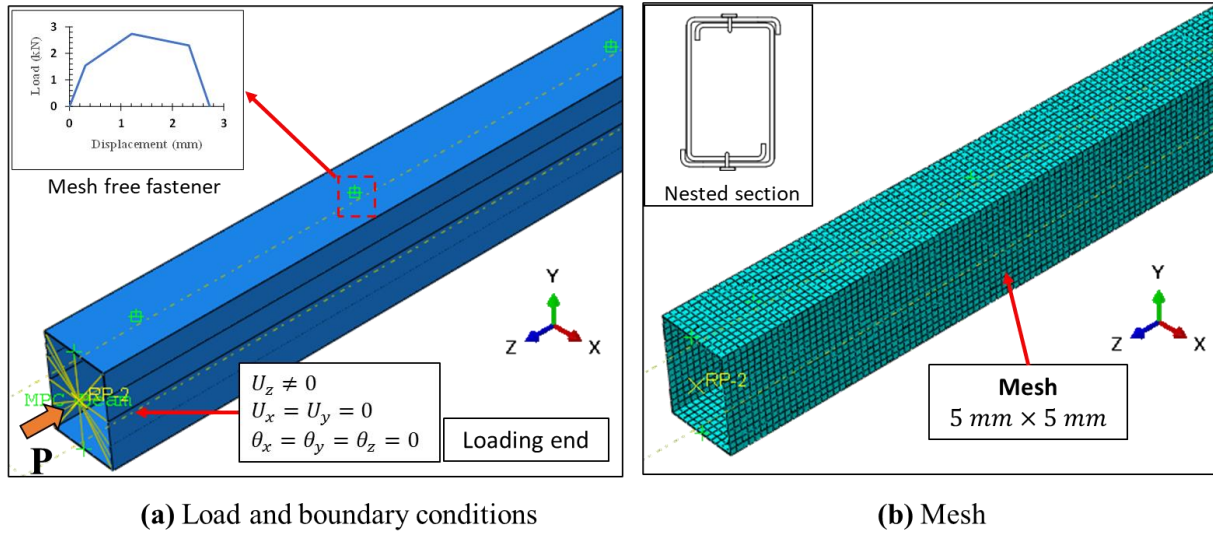


Figure 1: Finite element model of fixed-end built-up nested section adopted in the study

The material properties were included in the FE analysis using an incremental plasticity model where true stress and strain values were used. The imperfections were added to the FE model by performing linear perturbation or an Eigenvalue analysis. The Eigenvectors obtained from the linear perturbation analysis were scaled with an appropriate factor and added to the FE model for non-linear analysis. For flexural buckling mode, an imperfection factor of $L/1000$ was used, as suggested in AS/NZS-4600 (2018).

Two lipped channels are connected using fasteners to form a built-up nested section. In this study, the connectors were modelled as Cartesian based mesh-free fasteners (Fig. 1). The non-linear load-deformation values suggested by Phan and Rasmussen (2018) were also included in the fastener model as a backbone curve. In the FE model of the built-up nested section, contact properties were included at the top and bottom flanges such that the surfaces in contact do not penetrate. For this, surface-to-surface contact properties were selected with the finite-sliding tracking method, and normal hard contact was selected, allowing separation after contact. In the literature, the use of contact properties has been shown to cause convergence issues (Zhang and Young 2015, 2018). Hence, an additional energy dissipation factor of 0.0002 and a damping factor of 0.005 were used based on the suggestion of Zhang and Young (2015). In the end, the non-linear analysis was performed using the Newton-Rapson method to obtain the ultimate load and failure mode of built-up nested members.

4. Validation of FE Model

The FE model of built-up nested sections was developed as per the above-discussed procedure and validated using the experimental results of Young and Chen (2008) and Roy et al. (2019). The ultimate load results of the FE model were compared with the test results in Table 1, which shows that the FE model can predict the ultimate load of CFS built-up nested section columns accurately.

Table 1: Comparison of ultimate load results from test (P_{u-test}) and FE analysis (P_{u-FE})

Reference	Specimen ID	P_{u-test} (kN)	P_{u-FE} (kN)	$\frac{P_{u-FE}}{P_{u-test}}$
Young and Chen (2008)	T1.5L2200	212.50	215.6	1.01
	T1.5L3000	165.80	168.02	1.01
	T1.9L2200	288.70	301.02	1.04
	T1.9L3000	201.20	215.2	1.07
Roy et al. (2019)	B75-1500-1	88.40	89.14	1.01
	B75-1500-2	89.70	89.14	0.99
	B75-1500-3	91.40	89.14	0.98
	B75-1500-4	92.70	89.14	0.96
			Mean	1.01
			CoV	0.03

5. Numerical Investigation on the Flexural Behaviour of Nested Section Columns

A detailed numerical study was performed on the built-up nested section columns which fail by flexural buckling. The parameters selected for this study are presented below.

- Built-up sections made of two lipped channels were selected for the analysis. The lipped channels were made asymmetric with unequal flanges of appropriate widths to allow perfect nesting of sections, as shown in Fig. 2.
- Two types of lipped channel sections (LC1 and LC2) were selected in this study (Table 2).
- The length of the member was selected between 1000 and 4000 mm such that flexural buckling will be the critical buckling mode.
- The analysis was performed with the pin-end (SS) and fixed-end (CC) boundary conditions.
- Four different fastener spacings were selected for the analysis, i.e., $L/2$, $L/3$, $L/5$, and $L/10$.
- Yield stress (f_y) of 300 MPa was selected for the analysis.

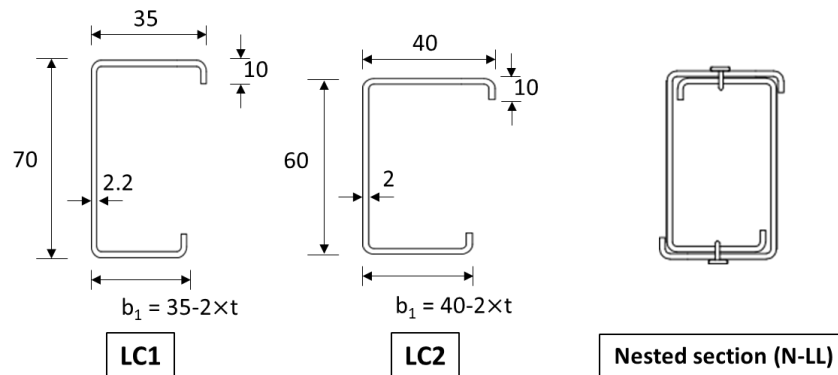


Figure 2: Built-up nested sections used in the numerical study

Table 2: Details of lipped channel sections used in the numerical study

Specimen ID	h (mm)	b (mm)	d (mm)	t (mm)	f_{crt} (MPa)	f_{crd} (MPa)
LC1	70	35	10	2.2	972.6	861.6
LC2	60	40	10	2.0	624.0	1055.0

The built-up nested sections used in the numerical study were labelled as shown in Fig. 3, including details of section type, web height, member length and fastener spacing. The results of the numerical study (64 nested sections) in terms of their ultimate load are presented in Table 3.

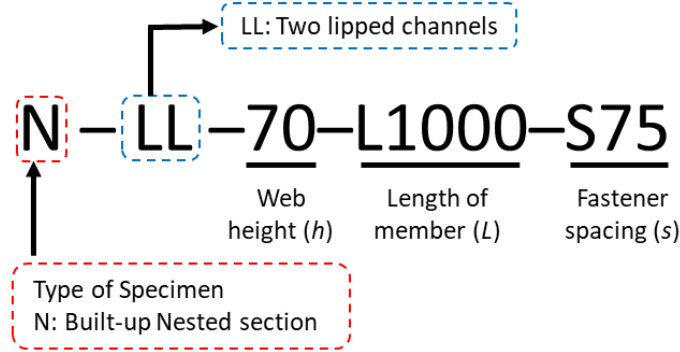


Figure 3: Labelling of nested sections used in the numerical study

Table 3: Ultimate load results (P_{u-FE}) and design strength prediction (P_{ng}) of nested sections used in the study

Sr. No.	Specimen label	Boundary condition ¹	$f_{crg-CoSFSM}$ (MPa)	P_{u-FE} (kN)	$\frac{P_{u-FE}}{P_{ng-CoSFSM}}$	$\frac{P_{u-FE}}{P_{ng-MSR}}$	$\frac{P_{u-FE}}{P_{ng-prop}}$
1	N-LL-70-L1000-S500	SS	367.72	182.57	1.23	1.32	1.06
2	N-LL-70-L2000-S1000	SS	94.00	58.99	1.05	1.24	0.92
3	N-LL-70-L3000-S1500	SS	41.85	27.20	1.08	1.28	0.95
4	N-LL-70-L4000-S2000	SS	23.61	15.52	1.09	1.30	0.96
5	N-LL-70-L1000-S333.3	SS	372.58	184.13	1.23	1.26	1.07
6	N-LL-70-L2000-S666.7	SS	95.27	59.21	1.04	1.08	0.91
7	N-LL-70-L3000-S1000	SS	42.46	27.35	1.07	1.12	0.94
8	N-LL-70-L4000-S1333.3	SS	23.97	15.74	1.09	1.15	0.96
9	N-LL-70-L1000-S200	SS	376.09	185.00	1.24	1.24	1.07
10	N-LL-70-L2000-S400	SS	96.00	59.24	1.03	1.00	0.90
11	N-LL-70-L3000-S600	SS	42.80	27.64	1.08	1.04	0.94
12	N-LL-70-L4000-S800	SS	24.16	15.78	1.09	1.06	0.95
13	N-LL-70-L1000-S100	SS	378.57	197.61	1.32	1.31	1.14
14	N-LL-70-L2000-S200	SS	96.43	59.71	1.03	0.97	0.90
15	N-LL-70-L3000-S300	SS	42.97	28.59	1.11	1.04	0.97
16	N-LL-70-L4000-S400	SS	24.25	16.06	1.10	1.04	0.97
17	N-LL-70-L1500-S750	CC	611.83	189.25	1.12	1.35	1.00
18	N-LL-70-L2000-S1000	CC	334.28	159.52	1.11	1.53	0.95
19	N-LL-70-L3000-S1500	CC	150.00	109.91	1.18	2.22	1.06
20	N-LL-70-L4000-S2000	CC	84.77	52.86	1.04	1.89	0.91
21	N-LL-70-L1500-S500	CC	667.50	197.89	1.15	1.25	1.04
22	N-LL-70-L2000-S666.7	CC	362.97	159.52	1.08	1.24	0.93
23	N-LL-70-L3000-S1000	CC	164.27	119.77	1.20	1.67	1.06
24	N-LL-70-L4000-S1333.3	CC	93.15	58.44	1.04	1.45	0.92

1. SS - Simply supported (Pin-ends) and CC- Clamped-Clamped (Fixed-ends)

Table 3: Contd.

Sr. No.	Specimen label	Boundary condition ¹	$f_{crg-CoSFSM}$ (MPa)	P_{u-FE} (kN)	$\frac{P_{u-FE}}{P_{ng-CoSFSM}}$	$\frac{P_{u-FE}}{P_{ng-MSR}}$	$\frac{P_{u-FE}}{P_{ng-prop}}$
					$P_{ng-CoSFSM}$	P_{ng-MSR}	$P_{ng-prop}$
25	N-LL-70-L1500-S300	CC	686.39	198.36	1.15	1.18	1.04
26	N-LL-70-L2000-S400	CC	373.11	169.29	1.13	1.18	0.98
27	N-LL-70-L3000-S600	CC	168.86	119.85	1.18	1.32	1.04
28	N-LL-70-L4000-S800	CC	95.80	73.52	1.28	1.41	1.12
29	N-LL-70-L1500-S150	CC	702.29	198.47	1.14	1.15	1.03
30	N-LL-70-L2000-S200	CC	381.29	179.24	1.19	1.20	1.03
31	N-LL-70-L3000-S300	CC	171.94	119.87	1.16	1.19	1.02
32	N-LL-70-L4000-S400	CC	97.41	79.91	1.37	1.34	1.20
33	N-LL-60-L1000-S500	SS	466.83	169.32	1.17	1.24	1.02
34	N-LL-60-L2000-S1000	SS	119.46	81.05	1.24	1.49	1.09
35	N-LL-60-L3000-S1500	SS	53.25	38.64	1.33	1.60	1.16
36	N-LL-60-L4000-S2000	SS	29.94	29.50	1.80	2.17	1.58
37	N-LL-60-L1000-S333.3	SS	471.18	178.98	1.23	1.26	1.08
38	N-LL-60-L2000-S666.7	SS	120.50	89.94	1.36	1.45	1.20
39	N-LL-60-L3000-S1000	SS	53.74	39.98	1.36	1.45	1.19
40	N-LL-60-L4000-S1333.3	SS	30.22	29.98	1.81	1.93	1.59
41	N-LL-60-L1000-S200	SS	474.39	179.21	1.23	1.24	1.08
42	N-LL-60-L2000-S400	SS	121.10	89.94	1.36	1.34	1.19
43	N-LL-60-L3000-S600	SS	54.02	39.98	1.35	1.34	1.19
44	N-LL-60-L4000-S800	SS	30.38	29.98	1.80	1.79	1.58
45	N-LL-60-L1000-S100	SS	476.70	184.78	1.27	1.26	1.11
46	N-LL-60-L2000-S200	SS	121.46	89.94	1.35	1.30	1.19
47	N-LL-60-L3000-S300	SS	54.16	47.51	1.60	1.54	1.41
48	N-LL-60-L4000-S400	SS	30.45	29.98	1.80	1.73	1.58
49	N-LL-60-L1500-S750	CC	755.95	176.2	1.10	1.27	1.00
50	N-LL-60-L2000-S1000	CC	441.04	169.23	1.18	1.53	1.04
51	N-LL-60-L3000-S1500	CC	198.41	118.32	1.15	2.04	0.99
52	N-LL-60-L4000-S2000	CC	111.90	62.44	1.02	1.92	0.89
53	N-LL-60-L1500-S500	CC	793.00	178.28	1.11	1.17	1.01
54	N-LL-60-L2000-S666.7	CC	465.10	176.75	1.22	1.37	1.07
55	N-LL-60-L3000-S1000	CC	210.61	118.44	1.11	1.46	0.95
56	N-LL-60-L4000-S1333.3	CC	119.08	72.49	1.11	1.56	0.98
57	N-LL-60-L1500-S300	CC	819.80	182.26	1.13	1.15	1.03
58	N-LL-60-L2000-S400	CC	474.48	177.84	1.22	1.27	1.07
59	N-LL-60-L3000-S600	CC	214.56	119.36	1.11	1.22	0.95
60	N-LL-60-L4000-S800	CC	121.31	73.98	1.11	1.25	0.98
61	N-LL-60-L1500-S150	CC	837.69	184.17	1.13	1.14	1.04
62	N-LL-60-L2000-S200	CC	481.68	178.11	1.22	1.23	1.07
63	N-LL-60-L3000-S300	CC	217.14	120.2	1.11	1.14	0.95
64	N-LL-60-L4000-S400	CC	122.64	74.70	1.11	1.11	0.98
				Mean	1.21	1.36	1.07
				CoV	0.15	0.20	0.15
				Max.	1.81	2.22	1.59
				Min.	1.02	0.97	0.89
				β ($\phi = 0.85$)	3.04	3.10	2.59
				ϕ ($\beta = 2.50$)	0.99	1.03	0.87

1. SS - Simply supported (Pin-ends) and CC- Clamped-Clamped (Fixed-ends)

The following subsections present a detailed discussion on the effect of fastener spacing and an evaluation of the elastic flexural buckling stress (f_{crg}).

5.1 Effect of fastener spacing

The effect of fastener spacings on the elastic flexural buckling stress (f_{crg}) and the ultimate load (P_{u-FE}) of built-up nested section columns using LC1 and LC2 lipped channel sections is presented in Figs. 4 and 5, respectively. The results show that the reduction in fastener spacing does not significantly affect the buckling stress and ultimate load values except in the case of N-LL-70-4000 member with the fixed-ends. The presence of fasteners around the section neutral axis during flexural deformation will not contribute to the buckling stress or ultimate load; hence, its effect can be neglected.

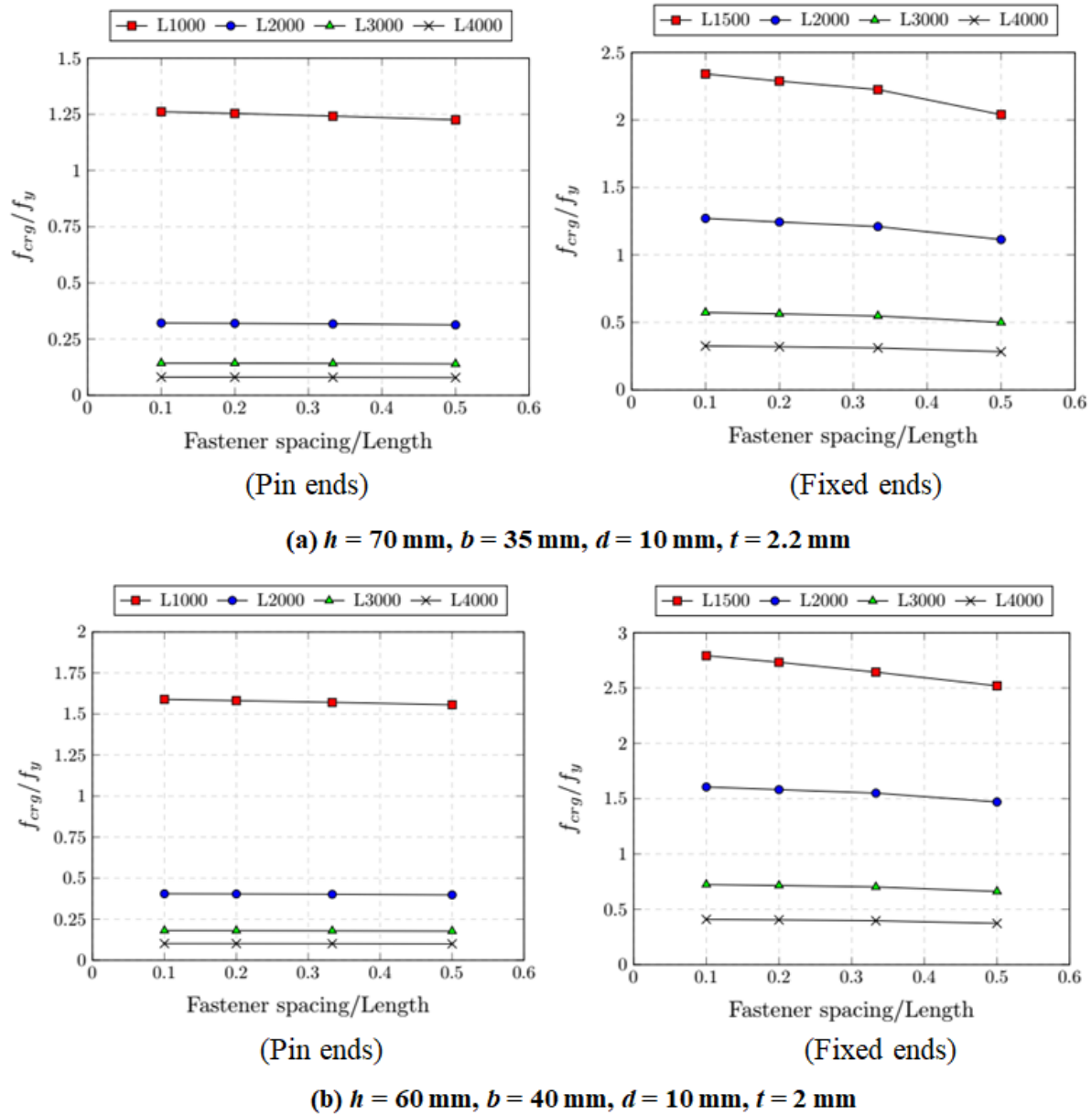


Figure 4: Effect of fastener spacing on the elastic flexural buckling stress (f_{crg}) of built-up nested section columns

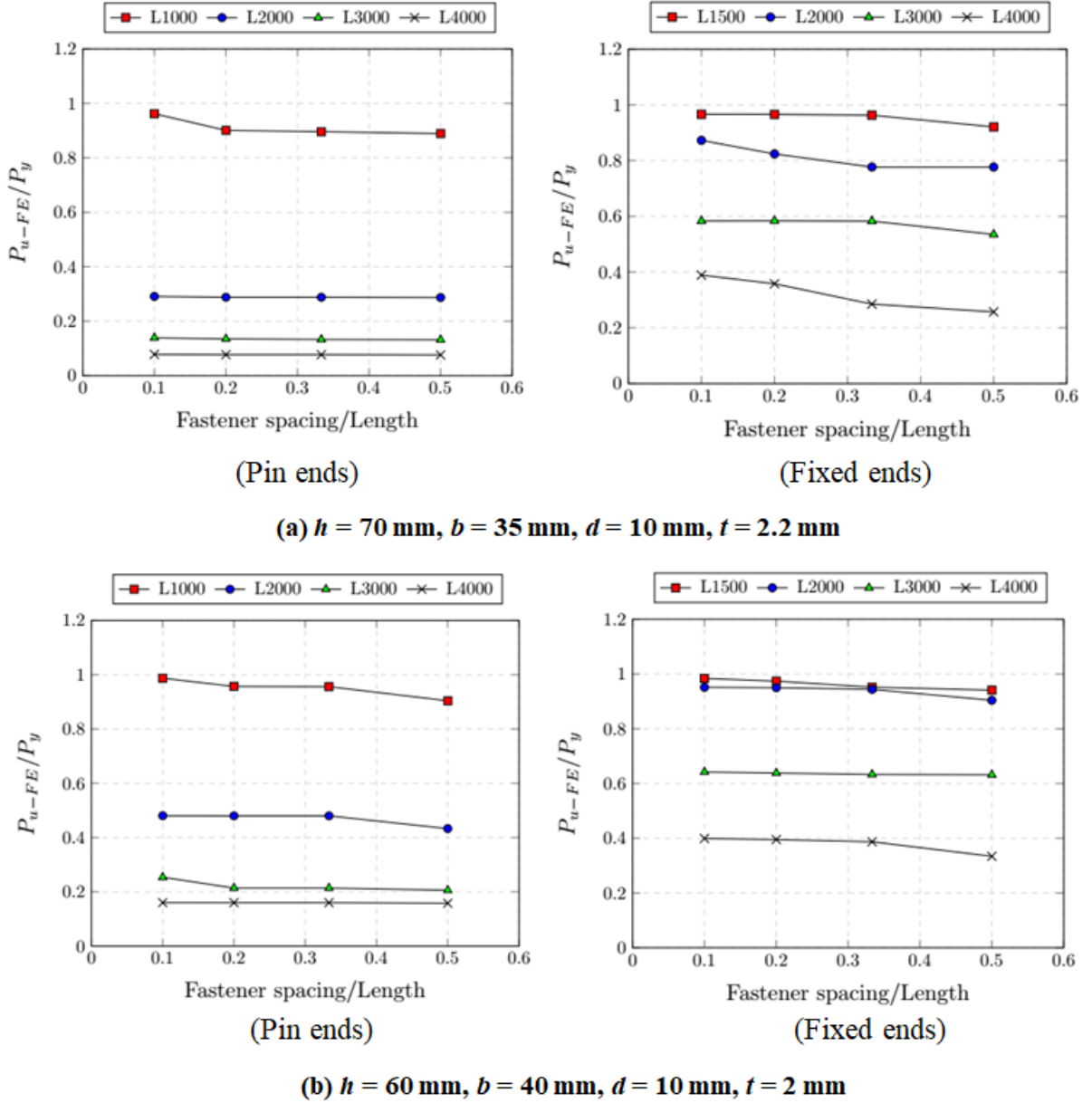


Figure 5: Effect of fastener spacing on the ultimate load (P_{u-FE}) of the built-up nested section columns

5.2 Elastic flexural buckling stress (f_{crg}) prediction

The elastic flexural buckling stress (f_{crg}) of the 64 nested sections were computed using the finite element (FE) models and compared with the buckling stress predictions of CoSFSM and the modified slenderness ratio (MSR) based method of NAS (2016). The comparison study reveals that the CoSFSM results match well with the FE results as the CoSFSM is developed to include the effect of fasteners. The mean of the ratio of results from CoSFSM to the FE analyses was 1.03 with a CoV of 0.05. The MSR based buckling stress predictions are less than the FE results as the MSR was developed for sections where screw fasteners experience shear during flexural deformations. Thus, the MSR may not apply to the elastic flexural buckling stress prediction of

built-up nested section columns. The mean of the ratio of MSR to the FE results was 0.90 with a CoV of 0.15. The results of the comparison study are presented in Fig. 6.

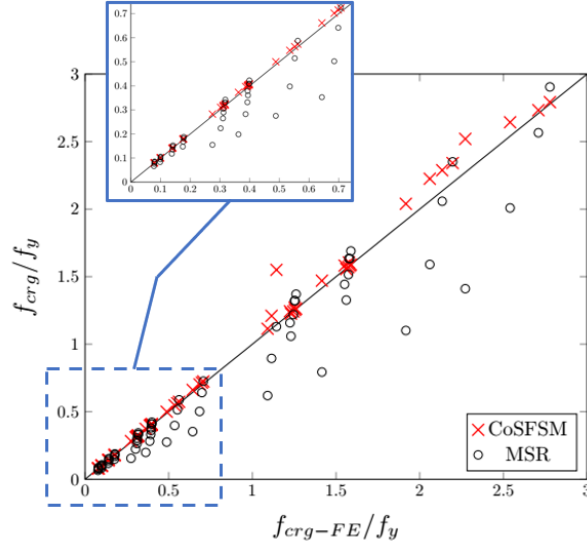


Figure 6: Comparison of elastic flexural buckling stresses (f_{cr_g}) obtained from CoSFSM and MSR with the FE results (f_{cr_g-FE})

As the MSR does not apply to the built-up nested section columns, an improved slenderness ratio (ISR) is proposed in this study based on the results of a statistical study. The proposed ISR is given as,

$$\left(\frac{KL}{r}\right)_{ISR} = \sqrt{\left(\frac{KL}{r}\right)_o^2 + 0.2 \times \left(\frac{KL}{r}\right)_o \left(\frac{s}{r_i}\right)} \quad (2)$$

The elastic flexural buckling stress results of the proposed ISR (f_{cr_g-ISR}) matched well with those of CoSFSM ($f_{cr_g-CoSFSM}$) as the mean of the ratio of the f_{cr_g-ISR} to $f_{cr_g-CoSFSM}$ was 1.01 with a CoV of 0.03. The results of the comparison study are presented in Fig. 7. As per the observations from Fig. 7, the MSR based buckling stress results matches closely with the actual buckling stress results when fastener spacing is small ($s/KL \leq 0.2$). The buckling stress behaviour will be closer to that of a fully-composite section at this fastener spacing. Also, the observations from Fig. 4 have shown that fastener spacing does not significantly affect the flexural buckling stress of built-up nested section columns. Hence, the proposed ISR is considered suitable for predicting the elastic flexural buckling stress of built-up nested section columns.

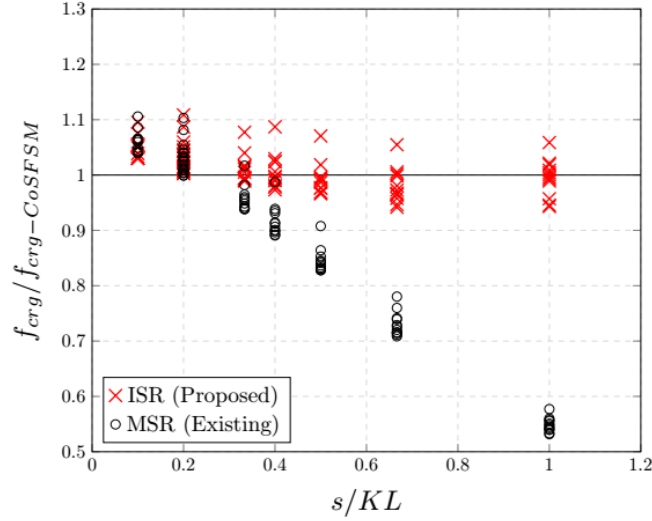


Figure 7: Validation of the proposed ISR using the buckling stress results of CoSFSM

In the next section, the DSM based global buckling design equations of NAS (2016) for the ultimate load prediction (P_{ng-DSM}) of the built-up nested section columns is evaluated with the actual buckling stress results of CoSFSM ($f_{crg-CoSFSM}$).

6. Design Strength Evaluation

As per the NAS (2016), the nominal flexural or global buckling strength (P_{ng-DSM}) shall be calculated as,

$$\text{For } \lambda_g \leq 1.5 \quad P_{ng-DSM} = (0.658\lambda_g^2)P_y \quad (3a)$$

$$\text{For } \lambda_g > 1.5 \quad P_{ng-DSM} = \left(\frac{0.877}{\lambda_g^2}\right)P_y \quad (3b)$$

where $\lambda_g = \sqrt{f_y/f_{crg}}$ and $P_y = f_y \times A_g$

The elastic flexural buckling stress predictions (f_{crg}) of CoSFSM and MSR were used here to calculate the values of λ_g . The DSM based design strength predictions (P_{ng-DSM}) are presented in Table 3, which are highly conservative when used with CoSFSM and MSR based flexural buckling stress (f_{crg}) results. The mean of the ratio of the FE results to the DSM-CoSFSM ($P_{ng-CoSFSM}$) and DSM-MSR (P_{ng-MSR}) results are 1.21 and 1.36, respectively. The built-up nested sections show high flexural buckling strengths even when actual buckling stress results are used in the evaluation.

As observed, the existing DSM based equation fails to predict the strength with good accuracy. Thus, a modified DSM-based flexural buckling equation for the ultimate load prediction of built-up nested section column can be developed.

The existing DSM-GB curve (Eq. 3) is composed of two curves,

- Curve-1: α^ζ , where $\zeta = \lambda_g^{\gamma_1}$, $\alpha = 0.658$ and $\gamma_1 = 2$, for $\lambda_g \leq 1.5$
- Curve-2: $\eta/\lambda_g^{\gamma_2}$, where $\eta = 0.877$ and $\gamma_2 = 2$, for $\lambda_g > 1.5$

Figure 8 shows the normalized FE strength and the DSM Curves-1 and 2 for different λ_g values. It shows that the FE results are higher than Curve-1 for small slenderness ($\lambda_g \leq 1.5$) and close to Curve-2 for large slenderness ($\lambda_g > 1.5$). Thus, a study is performed in Fig. 9, where α and γ_1 values are varied appropriately. The results show that for better strength prediction with the FE results, Curve-1 needs to be changed such that $\alpha > 0.658$ and $\gamma_1 > 2$.

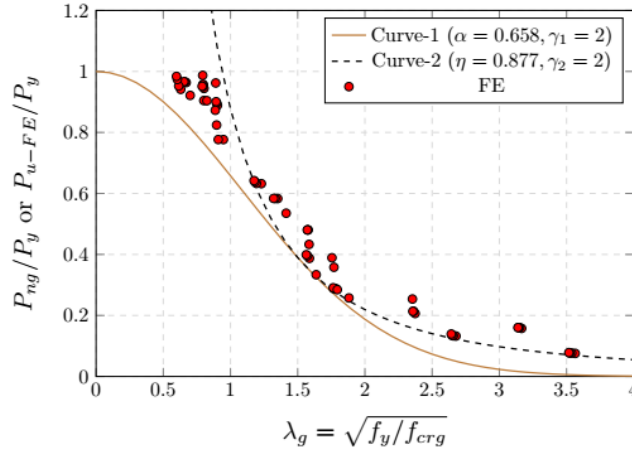


Figure 8: Plot of DSM-GB curves of NAS (2016) with the normalized FE ultimate load results (P_{u-FE}/P_y)

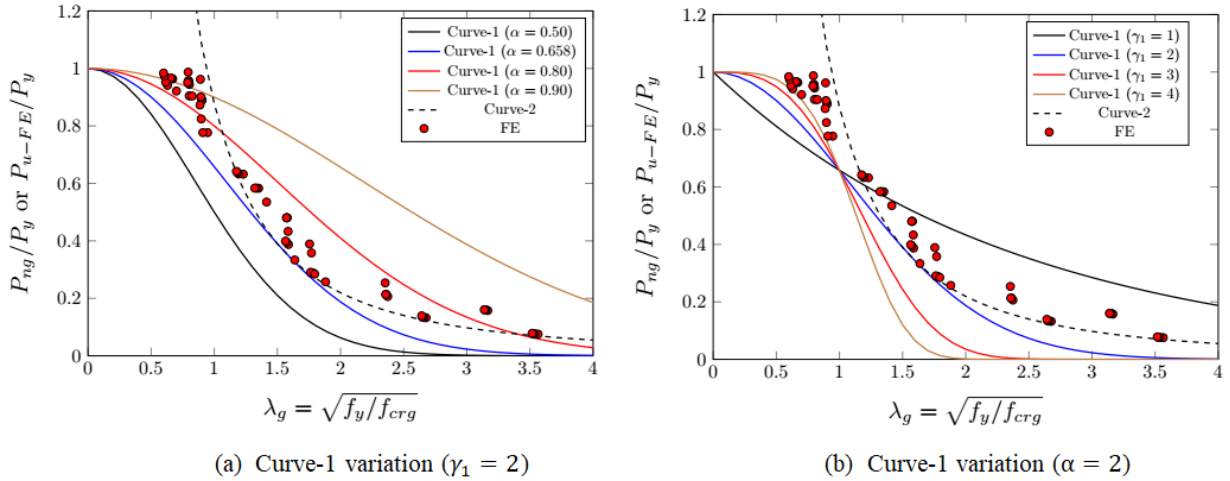


Figure 9: Effect of the variation of parameters on Curve-1

For Curve-2, a study is performed in Fig. 10, where η and γ_2 values are varied appropriately. The results show that for better strength prediction with the FE results, Curve-2 needs to be changed such that $\eta > 0.877$ and $\gamma_2 \leq 2$.

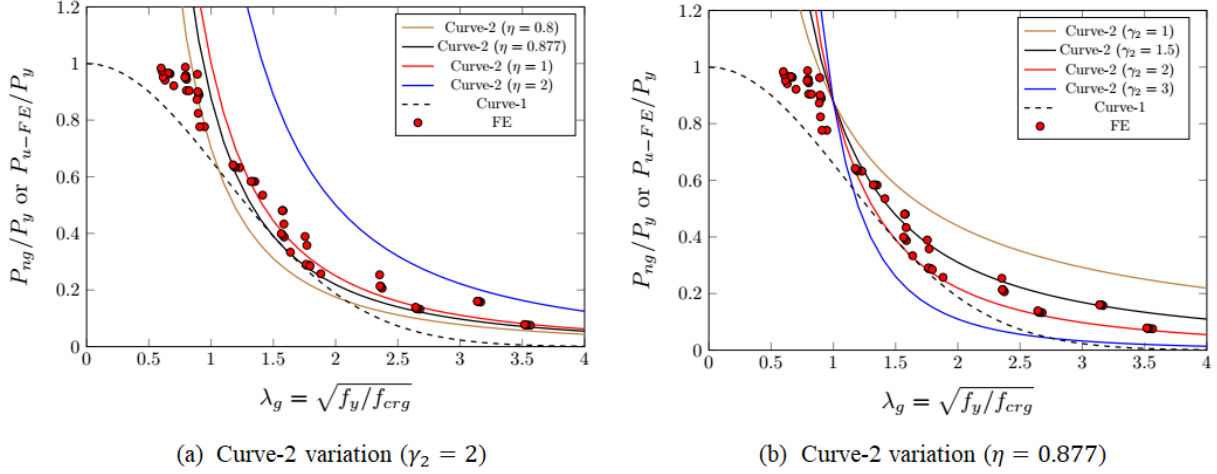


Figure 10: Effect of the variation of parameters on Curve-2

Based on the observations from Figs. 9 and 10, and the results of a detailed statistical study, a suitably modified DSM-GB curve is proposed. Equation 4 gives the proposed DSM-GB curve and is shown in Fig. 11 with FE results and the existing DSM-GB curve of NAS (2016). The proposed curve matches well with FE results (Table 3) as the mean of the ratio of the FE results (P_{u-FE}) to the proposed curve ($P_{ng-prop}$) is 1.07 with a CoV of 0.15. The proposed equation performs better than the existing DSM-GB equation, whose (P_{u-FE}/P_{ng-DSM}) mean value is 1.21 with a CoV of 0.15 (Table 3).

The proposed DSM-based flexural buckling strength equation can be given as,

$$\text{For } \lambda_g \leq 1.5 \quad P_{ng-prop} = (0.785\lambda_g^3)P_y \quad (4a)$$

$$\text{For } \lambda_g > 1.5 \quad P_{ng-prop} = P_y / \lambda_g^2 \quad (4b)$$

where $\lambda_g = \sqrt{f_y/f_{cr_g}}$ and $P_y = f_y \times A_g$

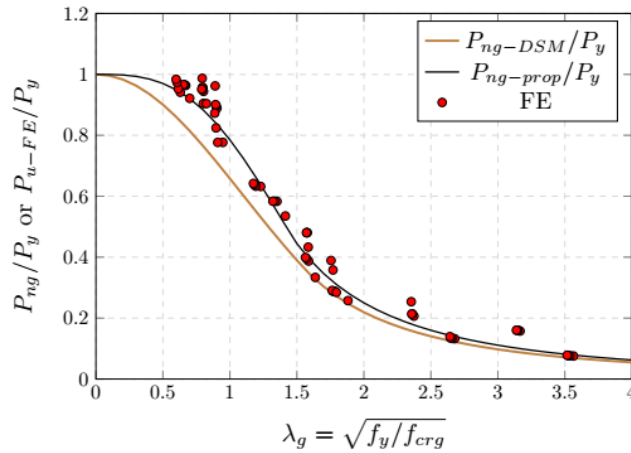


Figure 11: Plot of the proposed DSM-GB curve (Eq. 4) and comparison with the FE results

7. Reliability Study

The reliability of the proposed and existing DSM-GB equation should satisfy the target reliability index ($\beta_o = 2.50$) of NAS (2016) for LRFD. The reliability of the design procedures for the built-up nested section columns was investigated using the formulation given in Eq. 5. The value of resistance parameter $\phi = 0.85$ and other statistical parameters $M_m = 1.10$, $F_m = 1.00$, $V_m = 0.10$, $V_f = 0.05$, $V_q = 0.21$ were selected as suggested in Section K2.1.1-1 of NAS (2016). P_m and V_p are the mean and CoV values of the ratio of FE strength to the predicted strength. C_p is a correction factor, which is a function of the number of data samples considered in the analysis. The reliability factor (β) shall be calculated as,

$$\beta = \frac{\ln(1.52M_mF_mP_m/\phi)}{\sqrt{V_m^2 + V_f^2 + C_p V_p^2 + V_q^2}} \quad (5)$$

The reliability factor (β) of the proposed DSM-GB equation (Eq. 4) is 2.59 for a resistance factor (ϕ) of 0.85, which is higher than the target reliability index ($\beta_o = 2.50$). The reliability factor (β) of the existing DSM-GB equation (Eq. 3) is 3.04 for a resistance factor (ϕ) of 0.85, which is also higher than the target reliability index ($\beta_o = 2.50$). But the proposed DSM-GB equation (Eq. 4) shows economical results as the mean value of ($P_{u-FE}/P_{ng-prop}$) is close to one. The reliability factor (β) of the proposed DSM-GB equation (Eq. 4) when used with the proposed ISR (Eq. 2) is 2.58, as the buckling stress results of ISR are close to the actual buckling stress results of CoSFSM. Hence, the proposed design strength equation with the ISR will lead to economical and reliable designs.

8. Conclusions

In this study, the flexural buckling behaviour of the built-up nested section columns was investigated using a numerical study. The exact elastic flexural buckling stress (f_{crg}) solutions obtained using a compound spline finite strip-based computation tool, CoSFSM, show that the MSR will predict lower buckling stress results, which will lead to conservative strength predictions. Hence, an improved slenderness ratio (ISR) is proposed based on curve-fitting techniques, which shows matching results with the CoSFSM. The numerical study results show that the change in fastener spacing does not significantly affect the ultimate load results. Also, the existing DSM-GB equation of NAS (2016) predicts highly conservative strengths when used with the actual buckling stress results. Hence, a new DSM-GB equation is also proposed in this study. The proposed ISR and DSM-GB design equation will help the engineers obtain economical solutions for built-up nested section columns failing in flexural buckling.

Acknowledgements

The authors thank the Queensland University of Technology (Australia), Australian Research Council (Grant Number LP170100951) and Indian Institute of Technology Madras (India) for providing financial support and the infrastructure facilities for the research work.

References

- ABAQUS (2021). Analysis User's Manual-Version 6.21-1. ABAQUS Inc., USA.
- AISI S100 (2007). "North American Specification for the Design of Cold-Formed Steel Structural Members". American Iron and Steel Institute, Washington, DC, USA; 2007.
- AS/NZS-4600 (2018). "Cold-formed steel structures", Standards Australia/Standards New Zealand, NSW, Australia.
- Li, Y., Li, Y., Wang, S., and Shen, Z. (2014). "Ultimate load-carrying capacity of cold-formed thin-walled columns with built-up box and I section under axial compression". *Thin-Walled Structures*, 79, 202-217.
- Mahar, A. M., Jayachandran, S. A. (2021). "A Computational Study on Buckling Behavior of Cold-Formed Steel Built-Up Columns Using Compound Spline Finite Strip Method". *International Journal of Structural Stability and Dynamics*, 21(05), 2150064.
- Mahar, A. M., Jayachandran, S. A., Mahendran, M. (2021). "Global buckling strength of discretely fastened back-to-back built-up cold-formed steel columns". *Journal of Constructional Steel Research*, 187, 106998.
- NAS (2016). "North American Specification for the design of cold-formed steel structural members", North American Cold-Formed Steel Specification, American Iron and Steel Institute, AISI S100-16, Washington, DC, 2016.
- Phan, D., Rasmussen, K. (2018). "Cold-formed steel bolted and screw-fastened connections in shear". *In Proc., 8th Int. Conf. on Thin-Walled Structures*. Lisbon, Portugal: Univ. of Lisbon.
- Reyes, W., Guzmán, A. (2011). "Evaluation of the slenderness ratio in built-up cold-formed box sections". *Journal of Constructional Steel Research*, 67(6), 929-935.
- Roy, K., Ting, T. C. H., Lau, H. H., Lim J. B. (2019). "Experimental and numerical investigations on the axial capacity of cold-formed steel built-up box sections". *Journal of Constructional Steel Research*, 160, 411-427.
- Vy, S. T., Mahendran, M. (2021). "Behaviour and design of slender built-up nested cold-formed steel compression members". *Engineering Structures*, 241, 112446.
- Whittle, J., Ramseyer, C. (2009). "Buckling capacities of axially loaded, cold-formed, built-up C-channels". *Thin-Walled Structures*, 47(2), 190-201.
- Young, B., Chen, J. (2008). "Design of cold-formed steel built-up closed sections with intermediate stiffeners". *Journal of Structural Engineering*, 134(5), 727-737.
- Zhang, J.-H., Young, B. (2015). "Numerical investigation and design of cold-formed steel built-up open section columns with longitudinal stiffeners". *Thin-Walled Structures*, 89, 178-191.
- Zhang, J.-H., Young, B. (2018). "Finite element analysis and design of cold-formed steel built-up closed section columns with web stiffeners". *Thin-Walled Structures*, 131, 223-237.